The American Journal of Human Genetics, Volume *99*

Supplemental Data

Isolated and Syndromic Retinal Dystrophy Caused by Biallelic Mutations in *RCBTB1*, a Gene Implicated in Ubiquitination

Frauke Coppieters, Giulia Ascari, Katharina Dannhausen, Konstantinos Nikopoulos, Frank Peelman, Marcus Karlstetter, Mingchu Xu, Cécile Brachet, Isabelle Meunier, Miltiadis K. Tsilimbaris, Chrysanthi Tsika, Styliani V. Blazaki, Sarah Vergult, Pietro Farinelli, Thalia Van Laethem, Miriam Bauwens, Marieke De Bruyne, Rui Chen, Thomas Langmann, Ruifang Sui, Françoise Meire, Carlo Rivolta, Christian P. Hamel, Bart P. Leroy, and Elfride De Baere

SUPPLEMENTAL DATA

Supplemental Note: Case Reports

Case report S1. Clinical case report of family F1.

Family history. Two sisters V:1 and V:2 from a consanguineous Turkish family F1 (Figure 1) were followed in a pediatric endocrinology outpatient clinic. Family history showed a goiter at 38 years of age in the mother (IV:2) and the association of retinitis pigmentosa (RP), goiter, premature ovarian failure and slight intellectual disability in a maternal cousin (IV:3). Both sibs V:1 and V:2 also display RP and slight intellectual disability for which special education is required.

Sibling V:2. She presented at 10.3 years of age with a goiter and was complaining of tiredness. Her physical examination showed normal height (142 cm, 0.3 standard deviation score, SDS), normal body mass index (18 kg/m^2, 0.3 SDS) and a pre-pubertal stage. In addition, a low forehead and small teeth were observed. Thyroid ultrasound confirmed the goiter (right lobe 11 ml, left lobe 7 ml) and laboratory results showed normal TSH and fT4, elevated thyroglobulin (140 µg/L [RR 0-25]) reflecting the increased thyroid volume. Gonadotropins were normal for age. No thyroid autoantibodies were detected. Follow-up showed an increase in thyroid volume despite L-thyroxine treatment, requiring subtotal thyroidectomy at 15 years of age. Spontaneous pubertal development started at 12 years and menarche occurred at 14 years, followed by secondary amenorrhea. At 15 years, gonadotropin elevation (Luteinizing hormone LH 10.8; Follicle-stimulating hormone FSH 16.3 U/L) was noted along with undetectable anti-Müllerian hormone (AMH), indicating primary ovarian failure. Further increase in gonadotropins was noted at 15 years of age: LH 23.9 and

FSH 32.7 U/L. Oestroprogestative substitution was instituted. She developed overweight over the years.

Sibling V:1. The older sister presented with secondary amenorrhea at 16 years of age, after spontaneous pubertal development and menarche at 14 years of age. Her physical examination showed normal height (162.8 cm), overweight (BMI 25 kg/m2, 1.1 SDS), small teeth and a goiter. Gonadotropins were elevated (LH 29.7 and FSH 48.9 U/L). Thyroid function tests were normal except for slight thyroglobulin elevation (65 µg/L, RR 0-25), reflecting the increased thyroid volume. No thyroid autoantibodies were detected. Oestroprogestative substitution was instituted.

Supplemental Figures

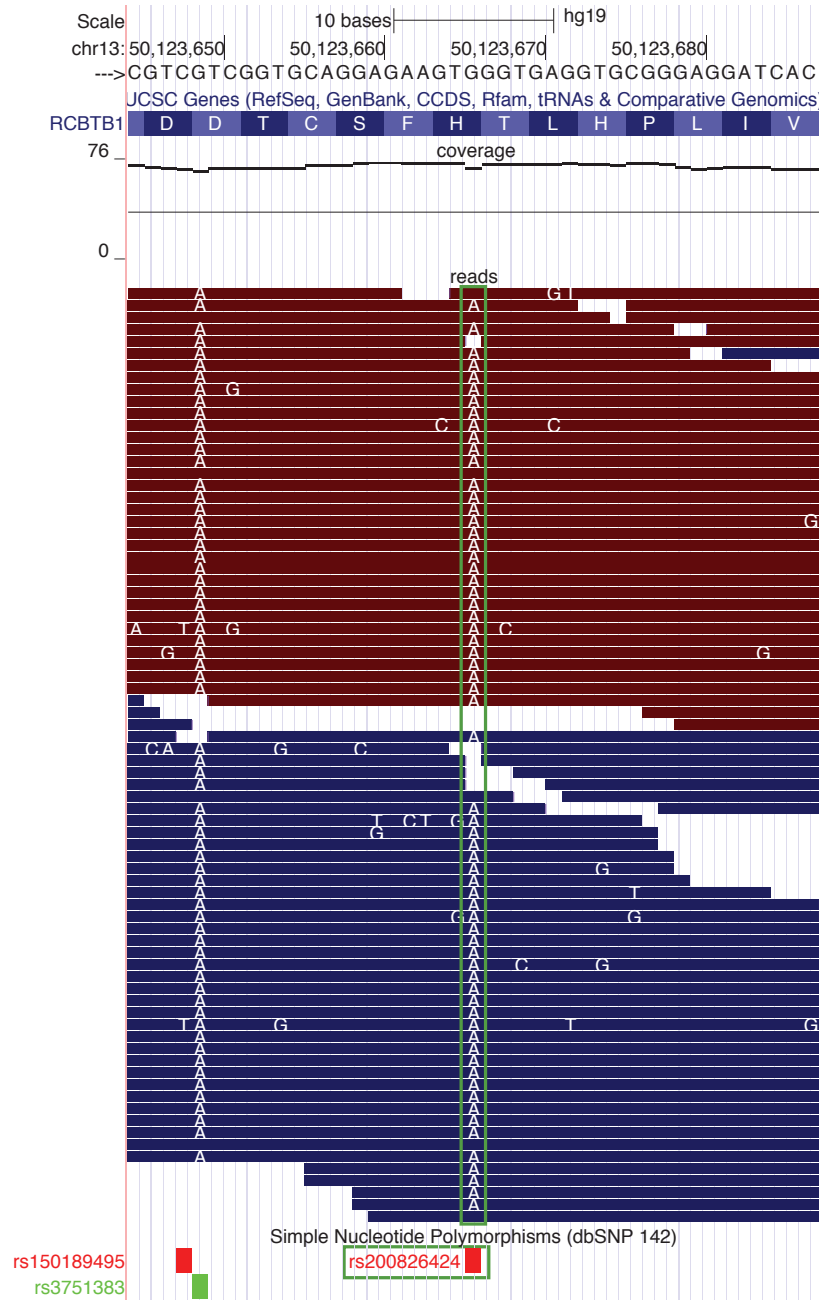

Figure S1. Sequence reads covering the *RCBTB1* mutation c.973C>T, p.(His325Tyr) (F1)

Whole exome sequencing (WES) yielded at least 20x coverage for over 91% of target regions (TruSeq Exome Enrichment, HiSeq 2000, Illumina). Read mapping, variant calling and annotation was performed with the CLC Genomics Workbench v. 6.0.4 (Qiagen). The coverage and variant allele frequency of the mutation were respectively 59x (V:1) and 72x (IV:3), and 98% (V:1) and 93% (IV:3). The mutation was confirmed by Sanger sequencing.

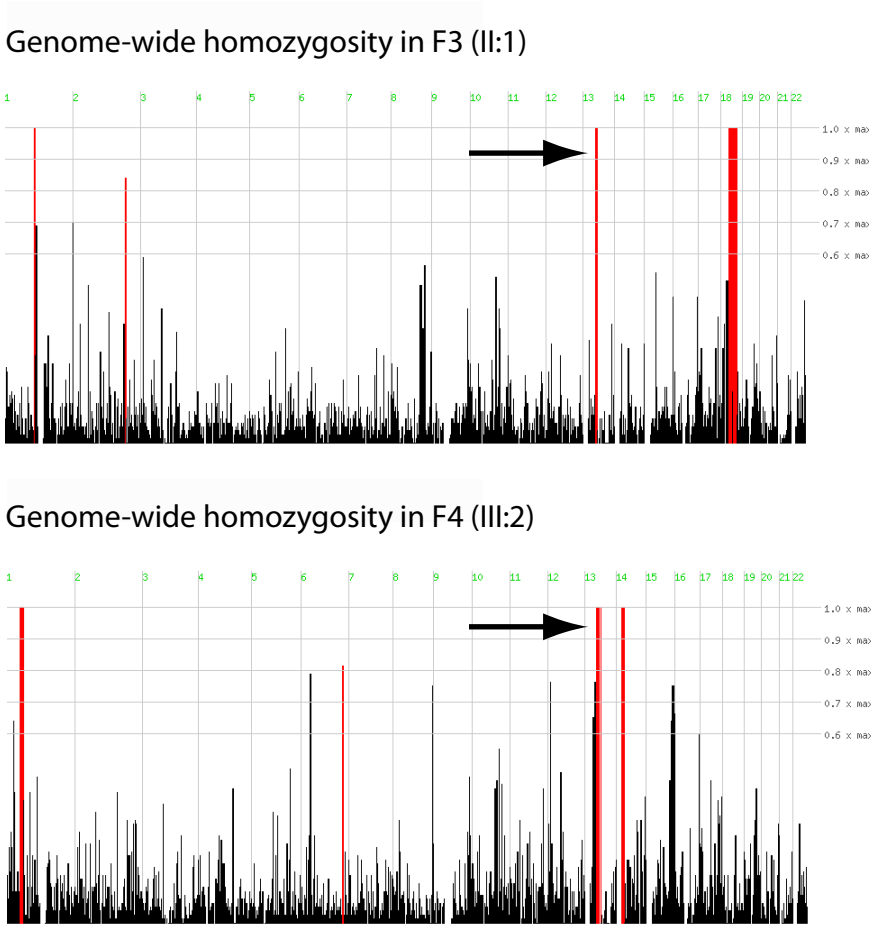

Figure S2. Homozygous regions in F3 and F4

Homozygosity mapping was performed on WES data (vcf files) using HomozygosityMapper. *RCBTB1* was located in the 3rd and largest homozygous region of F3 and F4, respectively (indicated with a black arrow).

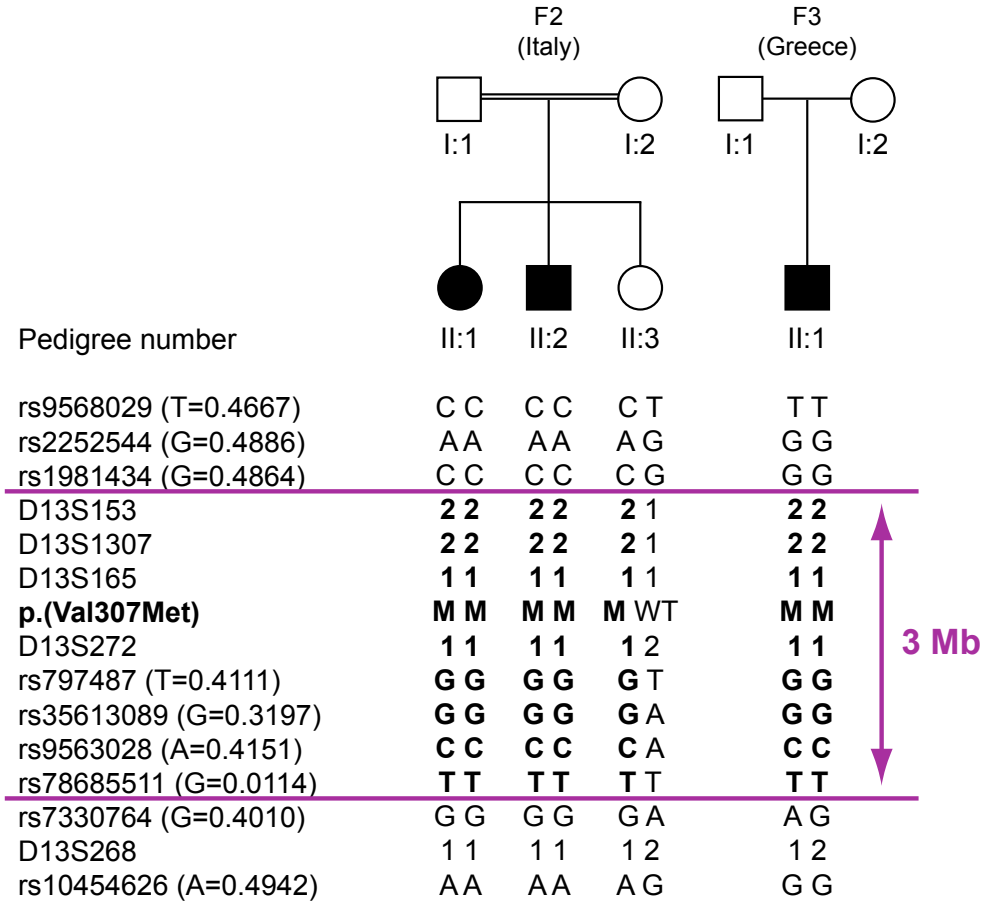

Figure S3. Haplotype analysis of the *RCBTB1* mutation c.919G>A, p.(Val307Met)

Segregation analysis of flanking microsatellites and single nucleotide polymorphisms revealed a common haplotype between the affected individuals of F2 and F3 with a maximal size of 3 megabases. For single nucleotide polymorphisms, the minor allele and its frequency are indicated between brackets.

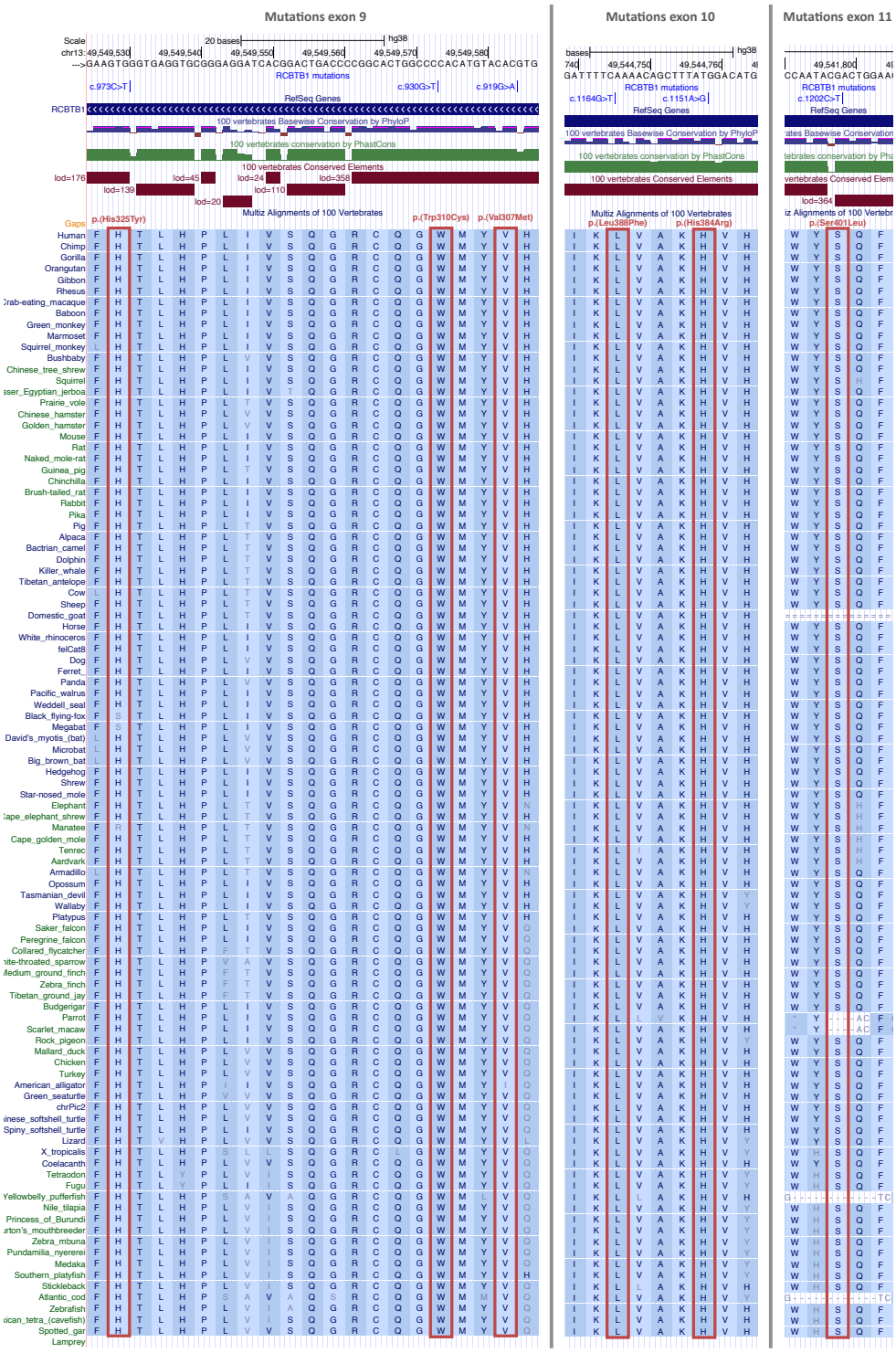

Figure S4. Nucleotide and amino acid conservation of identified *RCBTB1* missense mutations in 100 vertebrate species

Source: UCSC Genome Browser, Human GRCh38/hg38 assembly, Conservation track (Vertebrate Multiz Alignment & Conservation (100 Species)).

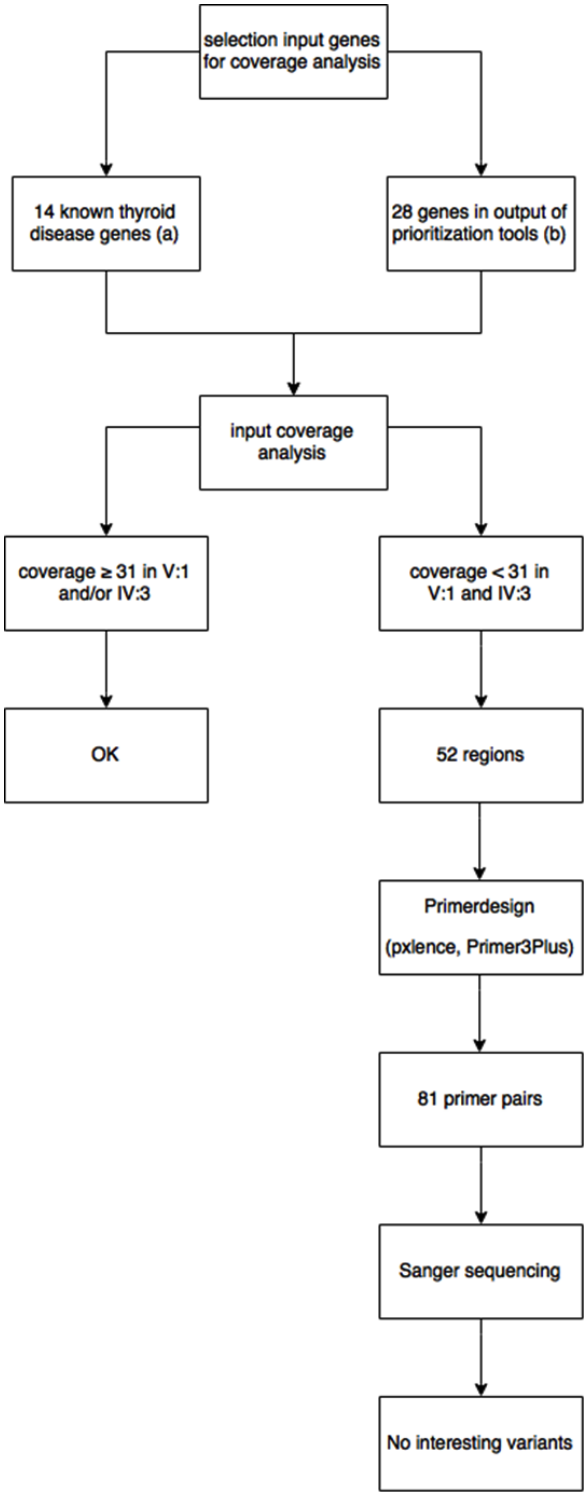

Figure S5. Sanger sequencing of thyroid related genes insufficiently covered by WES (F1)

Coverage analysis of a selection of genes was performed for individuals V:1 and IV:3. Input genes were selected based on the prioritization of thyroid disease genes: **(a)** training set, and **(b)** ranked genes lists (Table S5). Regions with coverage < 31x were analyzed with Sanger sequencing. No potential mutations were found that could explain the thyroid phenotype.

RCBTB1/Rcbtb1 and *CUL3/Cul3* expression in human and murine tissue

RCBTB1/Rcbtb1

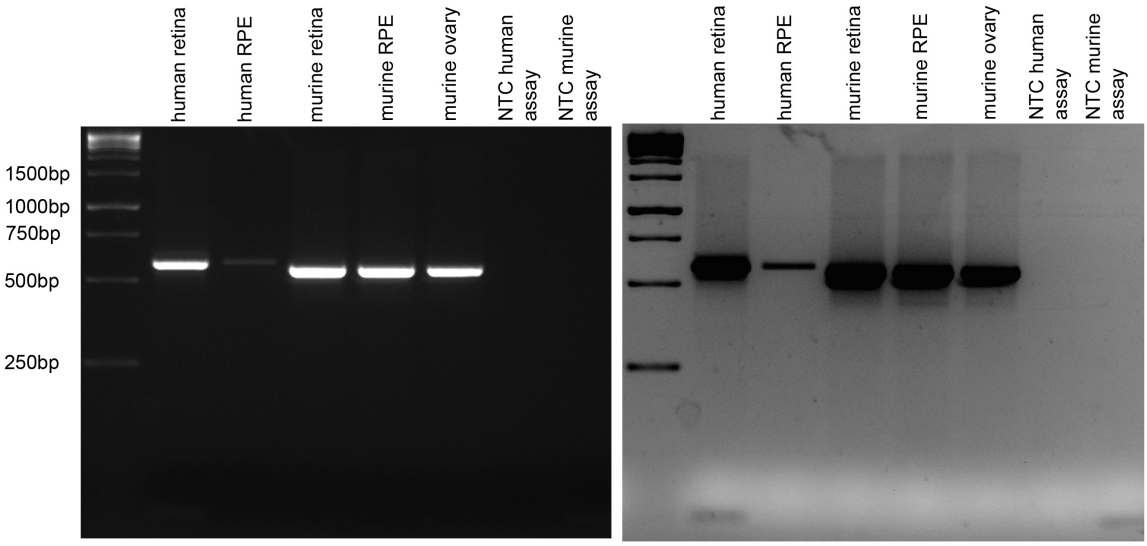

inverse image and higher exposure time

CUL3/Cul3

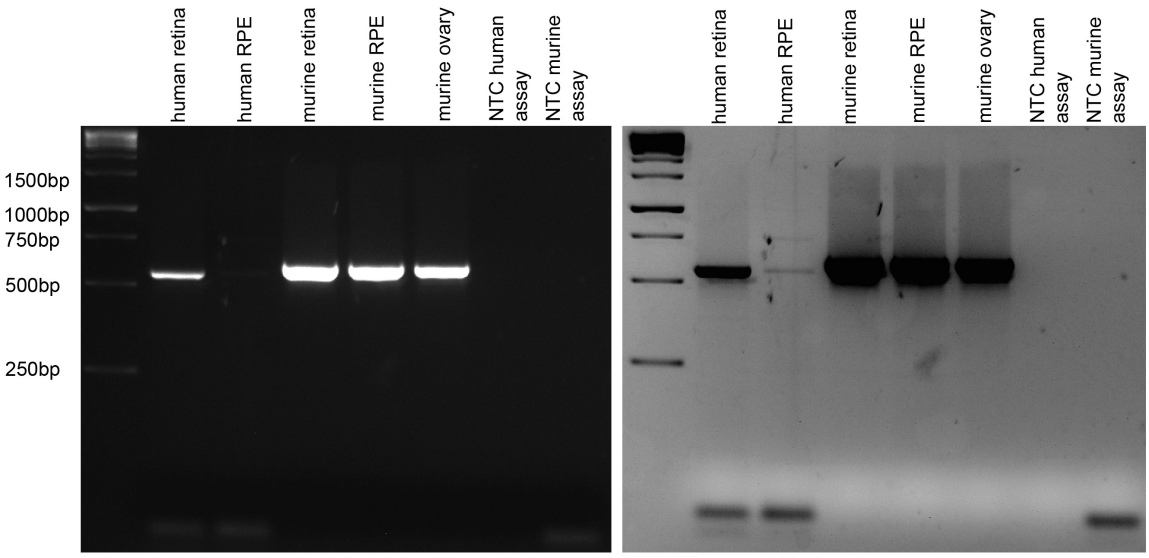

inverse image and higher exposure time

ACTB/Actb

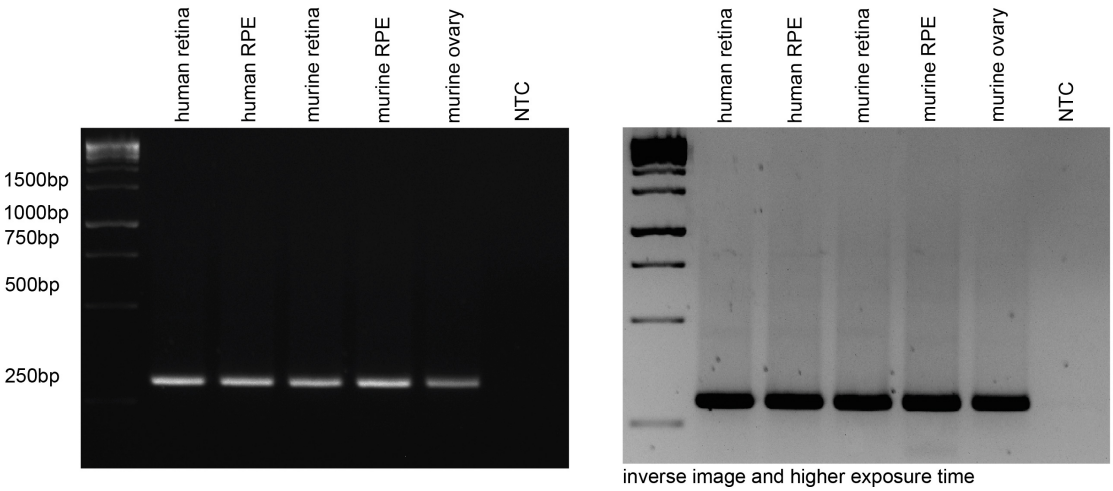

inverse image and higher exposure time

Figure S6. mRNA expression of *RCBTB1*/*Rcbtb1*, *CUL3*/*Cul3* and *ACTB*/*Actb* in human and murine tissues

RT-PCR of *RCBTB1*/*Rcbtb1* (upper panel) and *CUL3*/*Cul3* (middle panel) shows bands of expected size in human retina and RPE (weak), and in murine retina, RPE and ovary. *β-Actin* (*ACTB*/*Actb*, housekeeping gene) expression is shown in the lower panel. Human retina and RPE mRNA were extracted from an adult human donor (University of Cologne) and murine tissues from 10 weeks old C57BL/6 mice (4 retinas from 2 mice and 8 RPE from 4 mice).

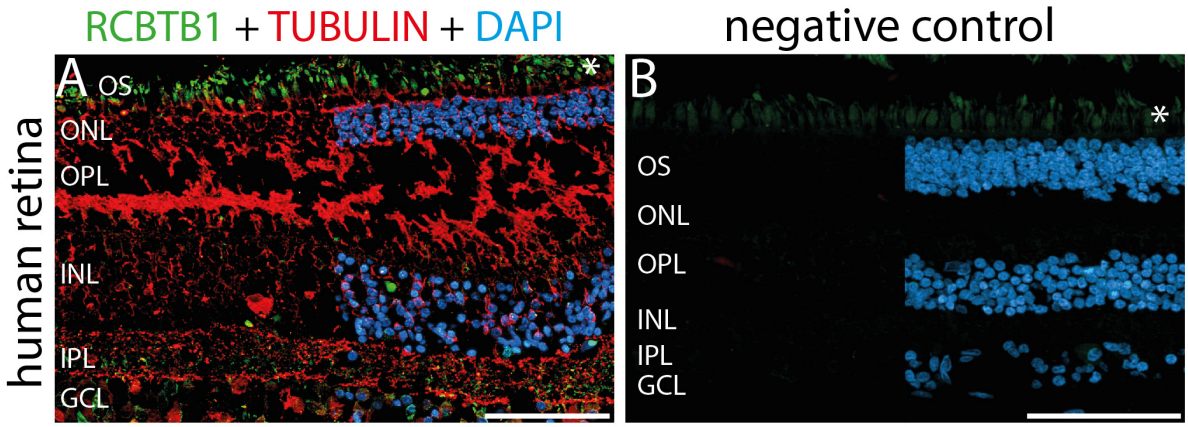

Figure S7. Co-staining of RCBTB1 and acetylated α tubulin

Left. Representative fluorescent images of horizontal paraffin-embedded cross-sections of human outer retina from donor eyes stained with anti-RCBTB1 antibody (green, 1:100, Abcam), anti-acetylated α tubulin (red, 1:250, Sigma Aldrich), and retinal counterstaining with 4',6-diamidino-2-phenylindole (DAPI) (blue). Immunohistochemistry was performed as described previously.[1] No clear ciliary co-localization could be observed. **Right. Control staining lacking primary antibody.** The green colour in the OS denotes autofluorescence of the photoreceptor cells (asterisks). Abbreviations used: OS, outer segments; ONL, outer nuclear layer; OPL, outer plexiform layer.

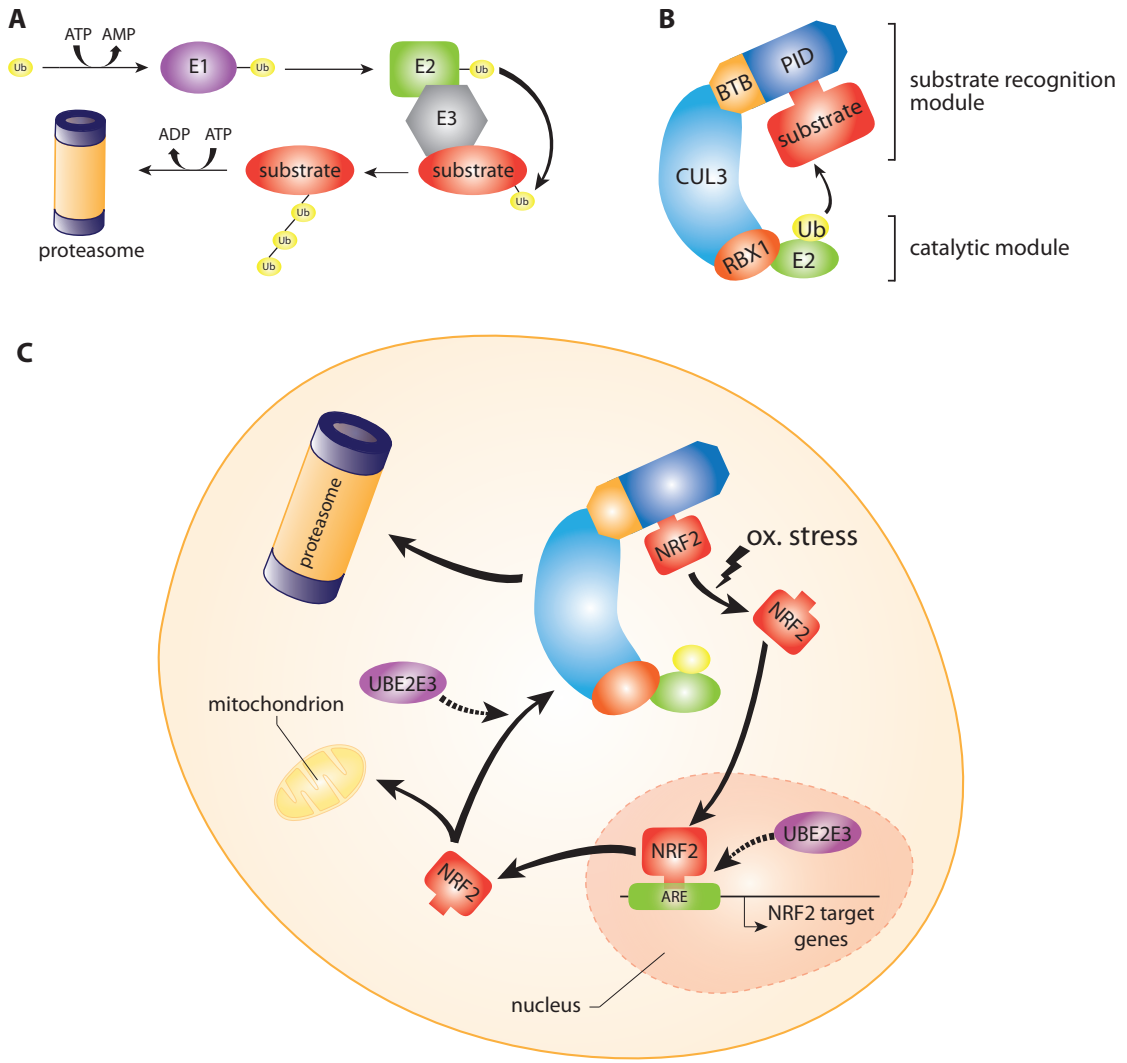

Figure S8. The role of different ubiquitination components in regulating NFE2L2 activity

A. The ubiquitin-proteasome pathway. **B.** The CULLIN3-RING ubiquitin ligase (CRL3) complex. In this complex, CUL3 serves a molecular scaffold between a catalytic module, composed of a RING finger domain protein (RBX1) recruiting an E2 enzyme, and a substrate recognition module. Substrate recognition is highly specific and is mediated by substrate adaptors such as RCBTB1, which bind CUL3 via a BTB domain and the substrate through a protein-protein interaction domain (PID). **C.** Simplified model of NFE2L2 (NRF2) regulation by a CRL3 complex and UBE2E3. Under basal conditions, NFE2L2 is polyubiquitinated by a CRL3 complex and degraded by the proteasome. Upon oxidative stress, NFE2L2 is released from this complex, translocates to the nucleus and binds antioxidant response elements (ARE), thus initiating gene transcription. Finally, NFE2L2 is localized to the cytoplasm (CRL3 complex) or mitochondria. UBE2E3 plays a role in both the activation and localization of NFE2L2. Figures adapted from [2-4].

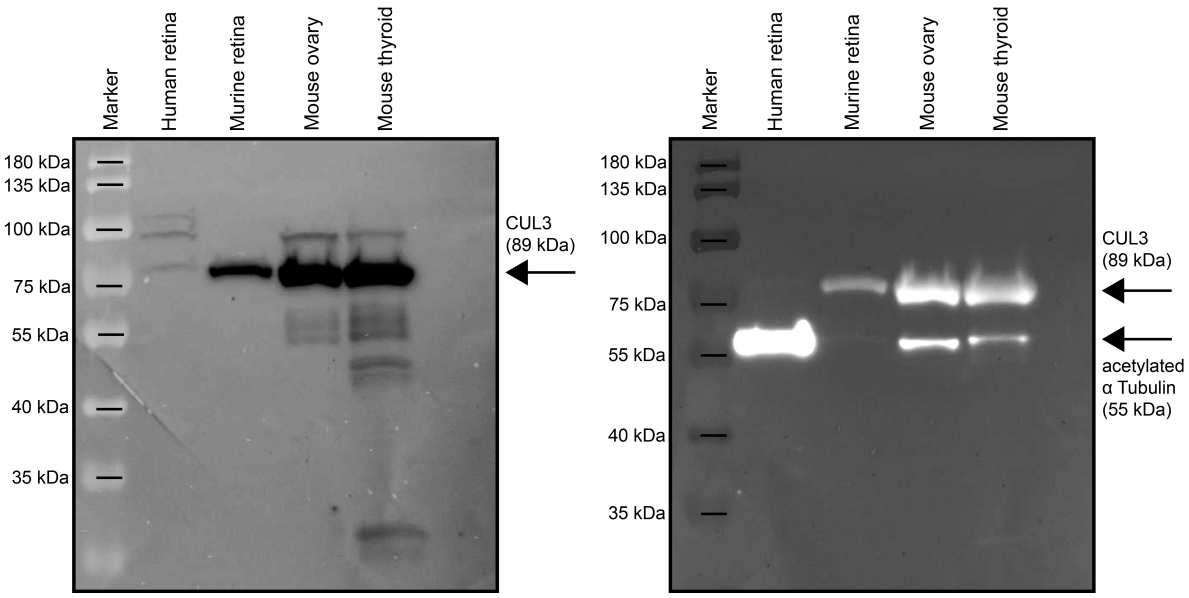

Figure S9. Western blot with CUL3 and α Tubulin antibody

Left. Western blot with anti-CUL3 antibody (Sigma) shows a weak band of 89 kDa in human retina and stronger bands in murine retina, ovary and thyroid. **Right.** Western blot with anti-acetylated α Tubulin (55 kDa, Sigma Aldrich) and anti-CUL3 (89 kDa) antibodies.

Supplemental Tables

Family	**F2, F3**	**F4**	**F1**	**F5**	**F6**	**F5**
gDNA Chr13(GRCh38)	g.49549584C>T	g.49549573C>A	g.49549530G>A	g.49544758T>C	g.49544745C>A	g.49541798G>A
gDNA Chr13(GRCh37)	g.50123720C>T	g.50123709C>A	g.50123666G>A	g.50118894T>C	g.50118881C>A	g.50115934G>A
cDNA	c.919G>A	c.930G>T	c.973C>T	c.1151A>G	c.1164G>T	c.1202C>T
Protein	p.(Val307Met)	p.(Trp310Cys)	p.(His325Tyr)	p.(His384Arg)	p.(Leu388Phe)	p.(Ser401Leu)
Exon	9	9	9	10	10	11
Domain/repeat	RCC1 6	RCC1 6	RCC1 6	BTB 1	BTB 1	BTB 1
dbSNP	rs368217569	/	rs200826424	rs143970072	/	rs556664001
ExAC	ALL:A=0.0025%	ALL:T=0.00083%	ALL:T=0.0091%	ALL:G=0.0075%	/	ALL:T=0.0025%
ESP	EA: T=0.01% - AA: T=0.00%	/	EA: A=0.02% - AA: A=0.00%	EA: C=0.00% - AA: C=0.02%	/	/
CADD: scaled C-score (raw C-score)	34 (7.285869)	34 (7.624610)	23.8 (4.129498)	26.1 (5.444564)	27.4 (5.887771)	24.1 (4.384951)
PhyloP	5.45	5.45	3.84	4.64	0.45	5.69
Grantham	21	215	83	29	22	145
Align GVGD	Class C15 (GV: 0.00 - GD: 20.52)	Class C65 (GV: 0.00 - GD: 214.36)	Class C65 (GV: 0.00 - GD: 83.33)	Class C0 (GV: 227.83 - GD: 28.42)	Class C0 (GV: 234.72 - GD: 21.82)	Class C0 (GV: 208.55 - GD: 106.06)
SIFT	Deleterious (score: 0)	Deleterious (score: 0)	Deleterious (score: 0)	Deleterious (score: 0)	Deleterious (score: 0)	Deleterious (score: 0)
Mutation Taster	Disease causing (p-value: 1)	Disease causing (p-value: 1)	Disease causing (p-value: 1)	Disease causing (p-value: 1)	Disease causing (p-value: 1)	Disease causing (p-value: 1)
PolyPhen-2	Probably damaging (0.999)	Probably damaging (1.000)	Probably damaging (0.972)	Probably damaging (1.000)	Probably damaging (1.000)	Probably damaging (0.982)
Splicing	No difference	No difference	No difference	No difference	No difference	No difference

Table S1. Population frequencies and *in silico* predictions of *RCBTB1* mutations identified

UniProt was used to look up protein domains (Q8NDN9). All other information with exception of the C-scores (CADD v1.3),[5] was derived from Alamut Visual version 2.7 rev. 1 (NM_018191.3).

Catalogue number	Amplicon context sequence (GRCh38)
PXL-A0073925	Chr13:49533970-49534317
PXL-A0073926	Chr13:49540669-49541087
PXL-A0073927	Chr13:49541599-49542276
PXL-A0073928	Chr13:49544581-49544980
PXL-A0073929	Chr13:49549331-49549678
PXL-A0073930	Chr13:49551171-49551552
PXL-A0073932	Chr13:49555433-49555778
PXL-A0073933	Chr13:49559700-49560134
PXL-A0073934	Chr13:49566520-49566937
PXL-A0073935	Chr13:49567005-49567433
PXL-A0285511	Chr13:49552130-49552481

Table S2. PCR assays used for sequencing of the coding region of *RCBTB1*

All coding regions of *RCBTB1* were sequenced in 281 iRD probands using pxlence targeted resequencing assays, followed by library preparation with the Nextera XT DNA Library Preparation Kit (Illumina) and sequencing on a MiSeq instrument (Illumina).[6] Other primer sequences used in this study are available on request.

Family	Individual	Enrichment kit - sequencer	Mean coverage
F1	V:1	TruSeq Exome Enrichment - HiSeq 2000 (Illumina)	97.2
	IV:3		121.6
F2	II:4	SureSelect Human All Exon V5 (Agilent) – HiSeq 2000/2500 (Illumina)	43
	II:5		42
	II:6		43
F3	II:1	SureSelect Human All Exon 50/51 Mb (Agilent) - HiSeq 2500 (Illumina)	52.97
F4	III:2	SureSelect Human All Exon 50/51 Mb (Agilent) - HiSeq 2500 (Illumina)	66.83
F5	II:6	SureSelect Human All Exon V5 (Agilent) – HiSeq 2000 (Illumina)	78
F6	II:2	SeqCap EZ Exome v3 (NimbleGen) - HiSeq 2000 (Illumina)	112.1

Table S3. Whole exome sequencing methods and mean coverage

Family	**Genotype**	**Gene (transcript)**	**cDNA**	**protein**	**Selection based on**	**Arguments in favor of exclusion**
F1	HOM	*COG3* (NM_031431.3) (MIM *606975)	c.1931-21del (rs558175293)	p.?	*In silico* predictions (splicing)	Homozygotes in ExAC; cDNA analysis of *COG3*
	HOM	*NEK3* (NM_001146099.1) (MIM *604044)	c.876_876+1insA (rs72514762)	p.Gln293Thrfs	*In silico* predictions (splicing)	Homozygous in healthy control individuals
F2*	No potential disease-causing variants identified					
F3	No potential disease-causing variants identified					
F4	No potential disease-causing variants identified					
F5*	HET	*CACNA2D4* (NM_172364.4) (MIM *608171)	c.2087A>G	p.His696Arg	*In silico* predictions (missense)	Population frequency (rs115228472)
	HET		c.2065A>G	p.Ile689Val	2nd variant in *CACNA2D4*	Population frequency (rs76224631)
F6	No potential disease-causing variants identified					

Table S4. Candidate variants in known or candidate iRD genes identified by whole exome sequencing

Abbreviations used: HET, heterozygous; HOM, homozygous. *Families F2 and F5 were selected for WES based on a common retinal phenotype (small atrophic spots in the macular area that tend to go to confluence), which appeared not to be linked to any known RD gene.

INPUT	**Prioritization tool**	**Endeavour**	**GeneDistiller**	**PosMed**	**ToppGene**	**G2D**
	Prior knowledge	Training set	Training set	Phenotype (goiter)	Training set	Training set
	Search space	Chromosomal position	Chromosomal position	Chromosomal position	Gene list	Chromosomal position
Ranked genes list						
OUTPUT	**1**	*RB1*	*ENOX1*	*CPB2*	*RB1*	*FNDC3A*
	2	*LCP1*	*COG3*	*RB1*	*HTR2A*	*ITM2B*
	3	*ITM2B*	*ATP7B*	*MLNR*	*NAA16*	*ATP7B*
	4	*AKAP11*	*RB1*	*TNFSF11*	*LCP1*	*TNFSF11*
	5	*ATP7B*	*CYSLTR2*	*CYSLTR2*	*GTF2F2*	*PCDH8*
	6	*HTR2A*	*HTR2A*	*HTR2A*	*ATP7B*	*LECT1*
	7	*INTS6*	*MLNR*	*ATP7B*	*ZC3H13*	*RB1*
	8	*TRIM13*	*TNFSF11*	*ITM2B*	*NAP1L4P3*	*GTF2F2*
	9	***RCBTB1***	*LPAR6*	*ESD*	*POLR2KP2*	*TSC22D1*
	10	*LECT1*	***RCBTB1***	*ARL11*	*LINC00562*	*COG3*

Table S5: Thyroid disease - prioritization of genes located in the IBD region of F1

Gene prioritization of genes located in the IBD region of F1 was performed using five tools. Data input is the chromosomal position of the IBD region (or the list of genes located in the IBD region) and the selected phenotype or the following training set: *NKX2-1, PAX8, FOXE1, GNAS, TSHR, TPO, TG, SLC5A5, SLC26A4, DUOX1, DUOX2, IYD*. Coordinates IBD region: chr13:41820714-53537171 (GRCh37/hg19). The first 10 hits of each output are shown.

Gene	gDNA (GRCh37)	cDNA	Protein	Transcript ID	Case samples				Predictions	Sanger sequencing			Conclusion
					Coverage		VAF			Confirmation in case samples	Segregation analysis	5 Control samples	
					V:1	IV:3	V:1	IV:3					
DUOX2 (MIM *606759)	chr15:45402883G>C	c.908C>G	p.P303R	NM_014080.4	77	78	39	29.5	AlignGVGD: C65 (GV:0.00-GD:102.71) SIFT: deleterious (score: 0) MutationTaster: disease causing (p-value: 1) Polyphen: probably damaging (1.000) Grantham:103 PhyloP: 5.45 dbSNP: rs151261408 ExAC: ALL: G=1.07% ESP: EA: C=1.77% - AA: C=0.25%	Confirmed (V:1 and IV:3)	- Present in affected individuals (V:1; IV3; IV:2) - Absent in affected individual (V:2) - Absent in healthy individuals (V:3; IV:1; III:5; III:6; IV:8; V:4)	Absent	Excluded: absent in affected individual (V:2) and present in normal controls[7]
*NEK3 (MIM *604044)	chr13:52718059dup	c.868dupA	p.R290fs*10	NM_001146099.1	50	43	70	72.1		Confirmed (V:1 and IV:3)	- Homozygous in affected individuals (V:1; IV:3; V2) - Heterozygous in affected individual (IV:2) - Absent in healthy individuals (V:3; IV:1; III:5; III:6; IV:8; V:4)	Homozygous in control sample	Excluded: homozygous in healthy control

Table S6: Analysis of thyroid related genes in WES data of F1

Variant interpretation was performed using Ingenuity Variant Analysis (IVA) ((QIAGEN, 2015 Release Spring) and Alamut Visual version 2.7 rev. 1. Segregation analysis in affected and healthy family members was performed when a variant was confirmed by Sanger sequencing in V:3 and IV:3. Abbreviation used: VAF, variant allele frequency.

Function	Name	Description
Synthesis and conjugation of glutathione	*GCLC* (MIM *606857)	Glutamate-cysteine ligase, catalytic subunit
	GCLM (MIM *601176)	Glutamate-cysteine ligase modifier subunit
	GSR (MIM +138300)	Glutathione reductase
	GSTA4 (MIM *605450)	Glutathione S-transferase alpha 4
	MGST2 (MIM *601733)	Microsomal glutathione S-transferase 2
Antioxidant	*PRDX1* (MIM *176763)	Peroxiredoxin 1
Drug metabolizing enzymes and transporters	*EPHX1* (MIM +132810)	Epoxide hydrolase 1
	NQO1 (MIM +125860)	NAD(P)H dehydrogenase, quinone 1
	ABCB6 (MIM *605452)	ATP binding cassette subfamily B member 6 (Langereis blood group)
	ABCC1 (MIM *158343)	ATP binding cassette subfamily C member 1
	SLC25A25 (MIM *608745)	Solute carrier family 25 (mitochondrial carrier; phosphate carrier), member 25
	SLC48A1 (MIM *612187)	Solute carrier family 48 (heme transporter), member 1
Metabolic enzymes	*IDH1* (MIM *147700)	Isocitrate dehydrogenase 1 (NADP+)
	LPL (MIM +609708)	Lipoprotein lipase
Heme and iron metabolism	*FECH* (MIM *612386)	Ferrochelatase
Transcription factors	*AHR* (MIM *600253)	Aryl hydrocarbon receptor
	HES1 (MIM *139605)	Hes family bHLH transcription factor 1
	RXRA (MIM *180245)	Retinoid X receptor alpha
	NOTCH1 (MIM *190198)	Notch 1
	YAF2 (MIM *607534)	YY1 associated factor 2
Cytokines	*IL6* (MIM *147620)	Interleukin 6

Table S7. NFE2L2 target genes investigated in this study

In total, 21 NFE2L2 target genes were selected from [8,9].

Target	p-value (corrected)	p-value	Ratio (controls/affected individuals)
RXRA	**0.000674**	0.000027	5.069
NFE2L2	**0.001116**	0.000089	2.917
IDH1	**0.002418**	0.000290	3.59
CUL3	**0.004803**	0.000769	1.635
SLC25A25	**0.025850**	0.005170	1.504
EPHX1	0.075750	0.018180	5.34
RBX1	0.137906	0.041600	1.625
HES1	0.137906	0.044130	0.197
NQO1	0.270778	0.097480	0.781
GCLC	0.336250	0.134500	1.127
AHR	0.367344	0.162600	1.784
ABCB6	0.367344	0.199200	2.417
MGST2	0.367344	0.206100	4.24
IL6	0.367344	0.223300	2.828
ABCC1	0.367344	0.226900	1.665
PRDX1	0.367344	0.235100	1.619
GSTA4	0.434853	0.295700	2.174
FECH	0.470875	0.367900	1.096
YAF2	0.470875	0.371000	2.605
LPL	0.470875	0.376700	3.722
GCLM	0.510341	0.445000	1.241
GSR	0.510341	0.449100	0.917
SLC48A1	0.859783	0.791000	1.16
NOTCH1	0.907083	0.870800	0.945
UBE2E3	0.982400	0.982400	0.989

Table S8. Statistical analysis on mRNA expression results

Statistical analysis was performed on log-transformed data using an unpaired t-test assuming unequal variances (qbase+, Biogazelle). Correction for multiple testing was performed using the multtest package (Bioconductor, R). The expression of five genes, indicated in bold, was significantly decreased in the group with 2 affected individuals in comparison with the control group (6 individuals) (p-value < 0.05). For the majority of the other genes, the ratio between the control group and group with affected individuals showed a trend of decreased mRNA expression in the affected individuals versus controls.

Supplemental References

1 Karlstetter, M. et al. (2014). Disruption of the retinitis pigmentosa 28 gene Fam161a in mice affects photoreceptor ciliary structure and leads to progressive retinal degeneration. Hum Mol Genet 23, 5197-5210.

2 Pagan, J., Seto T., Pagano M. & Cittadini A. (2013). Role of the ubiquitin proteasome system in the heart. Circ Res 112, 1046-1058.

3 Genschik, P., Sumara I. & Lechner E. (2013). The emerging family of CULLIN3-RING ubiquitin ligases (CRL3s): cellular functions and disease implications. EMBO J 32, 2307-2320.

4 Plafker, K.S. & Plafker S.M. (2015). The ubiquitin-conjugating enzyme UBE2E3 and its import receptor importin-11 regulate the localization and activity of the antioxidant transcription factor NRF2. Mol Biol Cell 26, 327-338.

5 Kircher, M., Witten D.M., Jain P., O'Roak B.J., Cooper G.M. & Shendure J. (2014). A general framework for estimating the relative pathogenicity of human genetic variants. Nat Genet 46, 310-315.

6 De Leeneer, K. et al. (2015). Flexible, scalable, and efficient targeted resequencing on a benchtop sequencer for variant detection in clinical practice. Hum Mutat 36, 379-387.

7 Muzza, M. et al. (2014). The clinical and molecular characterization of patients with dyshormonogenic congenital hypothyroidism reveals specific diagnostic clues for DUOX2 defects. J Clin Endocrinol Metab 99, E544-553.

8 Suzuki, T., Motohashi H. & Yamamoto M. (2013). Toward clinical application of the Keap1-Nrf2 pathway. Trends Pharmacol Sci 34, 340-346.

9 Al-Sawaf, O., Clarner T., Fragoulis A., Kan Y.W., Pufe T., Streetz K. & Wruck C.J. (2015). Nrf2 in health and disease: current and future clinical implications. Clin Sci (Lond) 129, 989-999.

Supplemental Web Resources

UCSC Genome Browser, https://genome.ucsc.edu
HomozygosityMapper, http://www.homozygositymapper.org
pxlence, https://www.pxlence.com
Primer3plus, http://primer3plus.com/cgi-bin/dev/primer3plus.cgi
UniProt, http://www.uniprot.org
CADD, http://cadd.gs.washington.edu
Online Mendelian Inheritance in Man, http://www.omim.org
Endeavour, http://homes.esat.kuleuven.be/~bioiuser/endeavour/tool/endeavourweb.php
GeneDistiller, http://www.genedistiller.org
PosMed, http://omicspace.riken.jp/PosMed
ToppGene, https://toppgene.cchmc.org/prioritization.jsp
G2D, http://g2d2.ogic.ca/index_known.html#use